



Comparing methods for estimating cranial capacity in incomplete human fossils using the Jingchuan 1 partial cranium as an example



Yameng Zhang^{a, b, *}, Xiujie Wu^a, Lynne A. Schepartz^{a, c}

^a Key Laboratory of Vertebrate Evolution and Human Origin of Chinese Academy of Sciences, Institute of Vertebrate Paleontology and Paleoanthropology, Chinese Academy of Sciences, Beijing 100044, China

^b Graduate University of Chinese Academy of Sciences, Beijing 100049, China

^c School of Anatomical Sciences, University of the Witwatersrand, Johannesburg, South Africa

ARTICLE INFO

Article history:

Available online 29 December 2015

Keywords:

Cranial capacity
Incomplete cranium
Endocast
Human fossils
Human evolution

ABSTRACT

Cranial capacity is one of the most important features used in hominin taxonomic and morphological analyses. For complete or nearly complete modern human crania, the traditional methods of estimating cranial capacity include filling the vault with seeds, the water displacement method, and the use of regression formulae based on craniometrics. For incomplete human fossils, cranial capacities are estimated by reconstructing endocasts manually or virtually or by using existing modern human skull regression formulae; however, the accuracies of these methods are usually dubious. To find a more accurate way of estimating cranial capacity of partial skulls, seven different estimation methods are compared, including the manual reconstruction of the endocast, models built on skulls and models built on endocasts. We then estimated the cranial capacity of a fragmentary Late Pleistocene cranium, Jingchuan 1. The models are tested on 30 modern human skulls, three *Homo erectus* fossils and one Late Pleistocene *Homo sapiens* fossil. In terms of estimating the cranial capacity of the fossil humans, our results indicate that the cranial capacity estimates based on endocasts are more precise than those from exterior skull dimensions, that multivariate models are better than univariate ones, and that the new models using PCR and PLSR have the smallest errors (<50 ml). From the seven methods, the cranial capacity of Jingchuan 1 is estimated to be 1630 ml, 1505 ml, 1533 ml, 1468 ml, 1512 ml, 1470 ml, and 1457 ml, respectively. The most reliable results for the Jingchuan 1 cranial capacity are between 1470 and 1457 ml, and the average is 1464 ml. This study has direct applications to future studies of cranial capacity variation and brain evolution in fossil and modern humans.

© 2015 Elsevier Ltd and INQUA. All rights reserved.

1. Introduction

Cranial capacity, the volume of the cranium interior, is used to represent brain size in morphometric studies. Cranial capacity is one of the most important comparative features in human evolutionary research. For complete modern human skulls, the methods commonly used to estimate cranial capacities include various packing methods employing seeds or other small objects, water displacement or volume measurement (Morton, 1849; Stewart, 1934; Tildesley, 1948; Ricklan and Tobias, 1986) or regression

formulae derived from modern skulls (Lee and Pearson, 1901; Olivier et al., 1978; Hwang et al., 1995).

In human fossils that are well-preserved and nearly complete, such as the Zhoukoudian *Homo erectus* specimens and the Liujiang 1 late Pleistocene *Homo sapiens* specimen, cranial capacities are estimated by reconstructing the endocasts manually or using CT technology (Weidenreich, 1936, 1937; Wu et al., 2008). However, for broken or incomplete specimens, the above methods are not useful, and many errors may be introduced due to poor preservation or the need to estimate landmarks. This often results in widely different estimates for the same specimen (Holloway, 2004, 1983, 1973). For example, the endocast of the australopithecine Stw-505 has been reconstructed many times, and its estimated cranial capacity ranges between 515 and 626 ml using different methods (Conroy et al., 1998; Lockwood, 1999). The 110-ml difference between the minimum and maximum estimates is >20% of the

* Corresponding author. Key Laboratory of Vertebrate Evolution and Human Origin of Chinese Academy of Sciences, Institute of Vertebrate Paleontology and Paleoanthropology, Chinese Academy of Sciences, Beijing 100044, China.

E-mail address: zhangyameng@ivpp.ac.cn (Y. Zhang).

potential capacity. Clearly, there is a need for more precise methods of cranial capacity estimation, and many mathematical models have been proposed.

The basic mathematical models include the simple linear regression model (SLR) and the multiple linear regression model (MLR), based on exterior skull or endocranial cast measurements (Cameron, 1928; Jorgensen and Quaade, 1956; Wolpoff, 1981). Formulae derived from external cranial measurements were the most popular methods because of their convenience (Isserlis, 1914; Hwang et al., 1995; Manjunath, 2002), but special structures on the cranium, such as superciliary arches, external occipital protuberance, and bone thickness, can cause inevitable errors in estimating the cranial capacity. Models based on endocast or endocranial measurements can eliminate this problem to a certain extent. Anthropologists first developed this correction technique using roentgenograms to obtain the length, width and height of the internal cranium (Hoadley and Pearson, 1929; Haack and Meihoff, 1971; Kaufman and David, 1972). However, in doing so, specialized equipment is needed and only a few chord lengths can be measured. With the development of CT technology, virtual endocasts were reconstructed, and more details on the surface of the endocast that used to be difficult to obtain from traditional morphometrics were acquired (Weber et al., 2000; Bruner et al., 2003). Additionally, the surface area and the volume are now easily quantified using 3D software applications (Márquez and Laitman, 2008; Isaza et al., 2014).

Traditional linear models have a drawback involving the selection of the variables. When dealing with multi-collinearity, the situation where many measurements are correlated with each other, it is very difficult to choose which variables to use or to

discard. A different selection of variables will make a difference in the ultimate prediction (Wold et al., 1984). To compensate for that issue, we also used Principal Component Regression (PCR) and Partial Least Squares Regression (PLSR) in building our models. PCR has many advantages over the traditional linear regression methods, including reducing the multi-collinearity, by analyzing more variables simultaneously. However, PCR only analyzes independent variables; thus, the extracted principle components may not truly reflect the relationship between the independent and dependent variables (Jolliffe, 1982; Carrascal et al., 2009). PLSR is quite similar to PCR, but it can offer further improvement for our purposes. PLSR is a relatively new multivariate statistical method that has developed rapidly in recent decades. This method was first developed in 1984 (Wold et al., 1984), and its principle basis is equivalent to principal component analysis and canonical correlation analysis (Geladi and Kowalski, 1986; Wang, 1999). As in canonical correlation analysis, PLSR also analyzes the relationship between the independent variables and the dependent variables. This means that the components extracted from the dependent variables are more related to the independent variable (Gil and Romera, 1998), i.e., cranial capacity in our study. Although PLSR has a short history, it has been used widely in many fields (Wold et al., 2001; Nguyen and Rocke, 2002; Liu et al., 2008). Its application to paleontology is rare, and this is the first trial use in paleoanthropology.

Jingchuan 1 is a partial human fossil cranium discovered in Niujiaogou, on the left bank of the Jingchuan river in Jingchuan County, Gansu Province (Liu et al., 1984). It was unearthed in dust-colored sandy clay associated with a typical Late Pleistocene mammalian fauna. The age of Jingchuan 1 is approximately 15 ka to

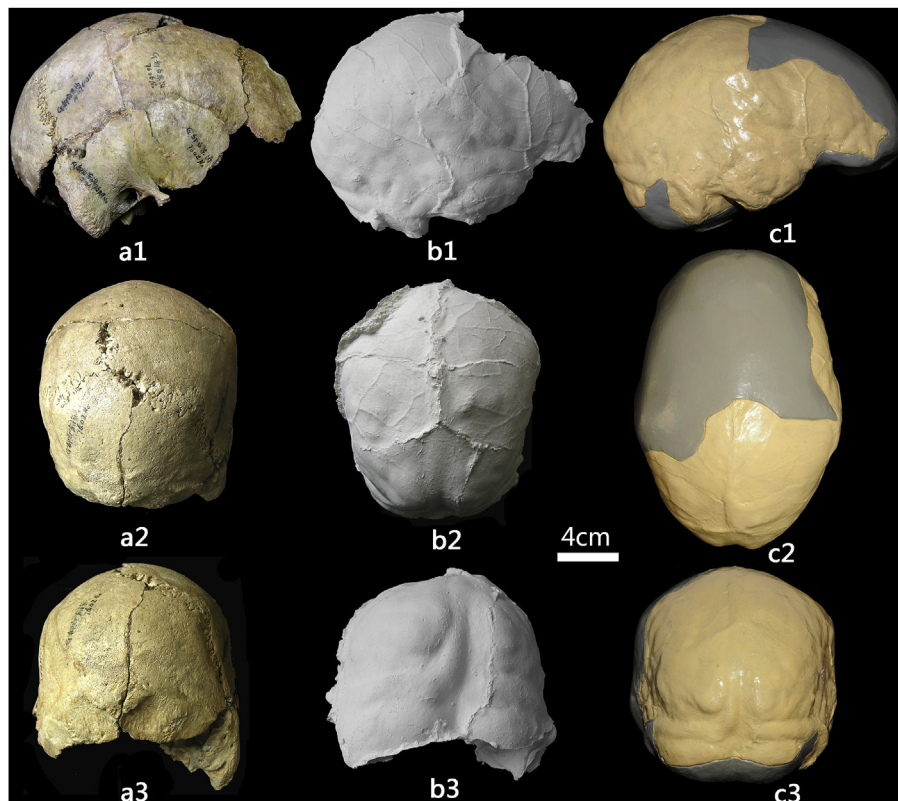


Fig. 1. The Jingchuan 1 cranium (a), the original endocast (b), and the full reconstructed endocast (c). a1, b1, c1: right lateral view; a2, b2, c2: posterior-superior view; a3, b3, c3: occipital view. The gray areas in c1–c3 are reconstruction.

48 ka based on the results of optically stimulated luminescence (OSL) dating (Li et al., 2010). Based on two existing cranial capacity formulae built on the single variables of porion-vertex and lambda-asterion, the Jingchuan 1 cranial capacity was estimated to be 1504 ml and 1545 ml, respectively (Li et al., 2010). Although the differences between the estimated cranial capacities are quite small, the accuracy of the measurements remains doubtful because only one variable was used. Thus, a re-estimation of the Jingchuan 1 cranial capacity is needed.

2. Materials and methods

2.1. Materials

The materials used in this study include the Jingchuan 1 cranium (Fig. 1) and comparative skulls and endocasts, which were used to build and test the cranial capacity models (Table 1). The Jingchuan 1 cranium is from the Jingchuan Museum of Gansu province. The endocast was reconstructed by Yameng Zhang and Xiujie Wu. To build the mathematical models for broken crania, eighty complete modern human skulls with endocasts and another twelve modern human endocasts were used (Table 1). These specimens were selected because they are from different modern human regional populations (including Africans, Europeans and Asians) and are therefore somewhat representative of the range of modern cranial capacity diversity. To test if the models can be used for *H. erectus* and Late Pleistocene *H. sapiens*, the well-preserved specimens ZKD X, XII, Hexian, and Predmosti 3 were chosen for comparison. Sixty of the modern human skulls and the four fossils casts, together with their endocasts, are from the collections of the Institute of Vertebrate Paleontology and Paleoanthropology (IVPP), Chinese Academy of Sciences; twenty skulls from different populations, with their endocasts, come from Holloway's (RLH) laboratory at Columbia University; and five Bantu, five Khoisan and two European endocasts are from the collections of the School of Anatomical Sciences, University of the Witwatersrand (Wits).

Table 1
Skulls and endocasts used for the model building and testing.

Specimen	N	Source
Chinese skulls and their endocasts	40 for modeling; 20 for testing	IVPP
Assorted skulls and their endocasts	10 for modeling; 10 for testing	RLH
Bantu endocasts	5 for modeling	Wits
Khoisan endocasts	5 for modeling	Wits
European endocasts	2 for modeling	Wits
ZKD X, ZKD XII, Hexian and their endocasts	3 <i>H. erectus</i> for testing	IVPP
Predmosti 3 skull and endocast	Late Pleistocene <i>Homo sapiens</i> for testing	IVPP

2.2. Endocast reconstruction

The Jingchuan 1 cranium preserves a small piece of the right frontal bone, a large posterior portion of the right parietal bone, an almost complete right temporal bone, a few left temporal bone fragments, a large portion of the occipital bone, and a small portion of the left parietal bone. The lambda region is complete. Beginning from lambda, the sagittal suture is approximately 5/6 preserved. The right coronal suture is represented by a 5-cm-long segment.

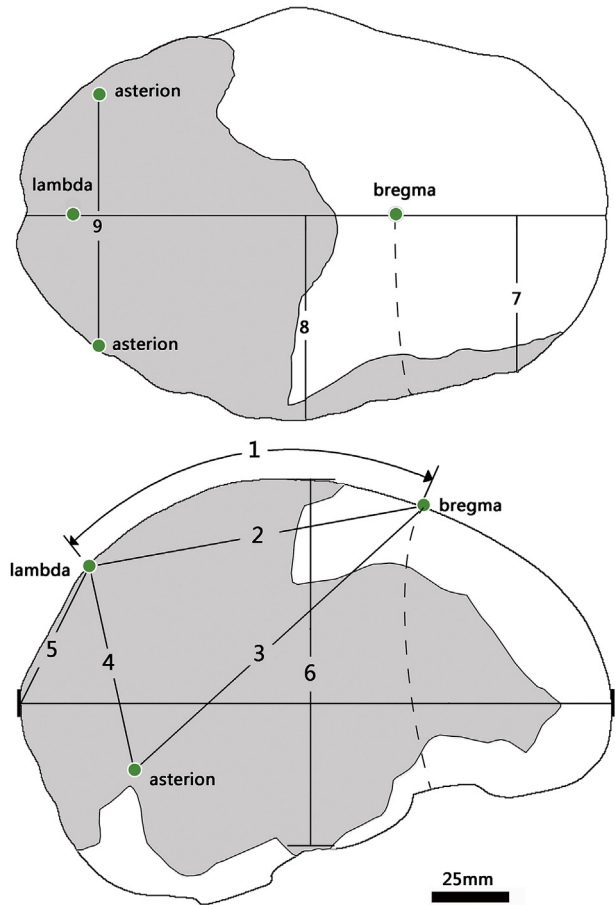


Fig. 2. Diagram of landmarks and measurements on endocasts.

The lambdoid suture is complete bilaterally (Fig. 1 a1–a3). Although bregma is missing, its location can be approximated by tracing the trajectories of the sagittal and coronal sutures.

A partial endocast was reconstructed based on the preservations of the cranium (Fig. 1 b1–b3). To help with the visualization, a modern endocast was used as reference to perform a complete reconstruction of the Jingchuan 1 endocast, including the shape of the cerebellum, the trajectories of the parietal and frontal lobes, and the pattern of the lateral part of the frontal lobe (Fig. 1 c1–c3). The endocast was first reconstructed using plasticine by hand. Then a mold was made using latex, and a plaster cast was made. The current morphometric study, however, only concerns the original endocranial areas, and the complete reconstruction must be considered as an aid to help visualization only.

2.3. Metric variables

According to the Jingchuan preservation, nine metric variables were chosen for the analysis (see details in Table 2 and Fig. 2). These variables are the bregma-lambda arc, bregma-lambda chord, bregma-asterion chord, lambda-asterion chord, lambda-occipital pole chord, asterion-asterion chord, brain height, maximum width of right frontal lobe, and maximum width of the right hemisphere. Among these, the bregma-asterion chord, lambda-asterion chord and lambda-occipital pole chord are measurable on both sides, and the mean was used as the final value (Fig. 2).

Table 2
List of metric variables on endocast with their definitions.

Measurement	Abbreviation	Description
1. Bregma-lambda arc	arc b-l	Parietal arc length, the arc distance between the internal bregma and the internal lambda on the endocast
2. Bregma-lambda chord	b-l	Parietal chord length, the chord distance between the internal bregma and the internal lambda on the endocast
3. Bregma-asterion chord	b-a	The distance between the internal bregma and the internal asterion on the endocast
4. Lambda-asterion chord	l-a	The distance between the internal lambda and the internal asterion on the endocast
5. Lambda-occipital pole chord	l-o	The distance between the internal lambda and the internal occipital pole on the endocast
6. Asterion-asterion chord	a-a	The distance between the two internal asterions on the endocast
7. Brain height	h	The vertical distance from temporal pole to the top of the endocast
8. Maximum width of right frontal lobe	w-f	The transverse distance from the most laterally protruding points of the frontal lobe to the middle sagittal plane
9. Maximum width of the right hemisphere	w-endo	The transverse distance from the most laterally protruding points of the endocast to the middle sagittal plane

2.4. Methods of cranial capacity estimation

We list the seven methods used to estimate cranial capacity in Table 3. Methods are divided into two categories, depending on whether they use measurements of skulls or endocasts. Their abbreviations are listed as used in the text.

Table 3
Methods of cranial capacity estimation used in this paper.

	Methods	Abbreviation
Skulls	a. Manual reconstruction	re-endo
	b. Simple linear regression	skull-pv
	c. Multiple linear regression	skull-mlr
Endocasts	d. Simple linear regression	endo-h
	e. Multiple linear regression	endo-mlr
	f. Principal component regression	endo-pcr
	g. Partial least squares regression	endo-plsr

2.4.1. Manual reconstruction of the endocast (re-endo)

The cranial capacity is directly estimated from the manually reconstructed endocasts using water displacement.

2.4.2. Simple linear regression model on skulls (skull-pv)

We used the porion-vertex (skull-pv) formula, $cc = 20.64963p-v - 973.261$ (Ding et al., 1992), which was employed in the previous study on the Jingchuan 1 cranium (Li et al., 2010), to test its accuracy for the specimens in this analysis. Twenty Chinese skulls and ten assorted skulls are used for testing (Table 1).

2.4.3. Multiple linear regression model on skulls (skull-mlr)

Forty Chinese and ten assorted skulls (Table 1) were used as modeling data. Only a few variables can be measured on Jingchuan 1, including the bregma-asterion (b-a), porion-vertex (p-v), and asterion-asterion (ast-ast). Their correlations with cranial capacity were found to be 0.76, 0.70, and 0.55, which are in a quite

reasonable range. Thus, all three were used as the dependent variables. The formula is as follows:

$cc = -1260.84 + 8.939 * p-v + 7.825 * b-a + 5.255 * ast-ast$, with an adjusted R-squared value of 0.68.

Testing data are the twenty Chinese skulls and ten assorted skulls (Table 1). An adjusted R-squared value is more suitable here because it reduces the over-fitting caused by the increased number of variables (Mevik and Cederkvist, 2004).

2.4.4. Simple linear regression model on endocasts (endo-h)

Landmarks that can be located on the Jingchuan 1 endocast include the bregma, lambda, asterion, temporal lobe, occipital lobe, the highest point of the endocast, the widest point of the right frontal lobe, and the widest point of the right hemisphere (Fig. 2). Brain height (h) has a relatively high correlation with cranial capacity, and it also resembles the porion-vertex height on a skull. To compare this formula with the porion-vertex formula, we chose this variable and built the following simple linear model: $cc = 18.92 * h - 775.88$. The adjusted R-squared value is 0.64. Sixty two modern human endocasts are used as modeling data, with the remaining thirty endocasts for testing (Table 1).

2.4.5. Multiple linear regression model on endocasts (endo-mlr)

The data were analyzed in R (R Core Team, 2015). After the multiple linear model was built, a stepwise method was used and the Akaike information criterion (AIC) was used to eliminate the redundant variables (Johnson and Wichern, 1992). Based on this process, the bregma-asterion (b-a), temporal lobe height (h), and width of the right hemisphere (w-half) were selected to build the model. The regression model is as follows:

$cc = 9.39 * b-a + 9.73 * h + 10.59 * w-half - 1600$, and the adjusted R-squared value is 0.83. Sixty two modern endocasts are used as modeling data, and the other thirty endocasts for testing.

2.4.6. Principal components regression model on endocasts (endo-pcr)

The data were analyzed in R (R Core Team, 2015), and the package “pls” (Mevik et al., 2013) was used. The function “pcr” was used to perform a PCR analysis, including a PCA and a regression. PCA was first performed on the training data, then the regression was performed from cranial capacity to principal components as calculated in the previous analysis. In order to determine the components that are needed in this analysis, cross validation was used to calculate the RMSEP (root mean squared error of prediction) (Mevik and Wehrens, 2007), and the R-squared value was calculated at the same time (Fig. 3). In Fig. 3, the first row is the increase of R-square through components and the second row is the change of RMSEP through the components. According to these two parameters, the first two components were chosen to build the model, and the R-squared value is 0.81. The sixty two modern endocasts from different regions are used as modeling data and the remaining thirty endocasts were used for testing (Table 1).

2.4.7. Partial least squares regression model on endocasts (endo-plsr)

The procedure for the partial least squares regression model is almost the same as that of the principal component regression, except the function here used in R is “plsr” (Mevik and Wehrens, 2007). Function “plsr” is used to perform a PLSR, including a PLS and a regression. PLS analysis is first performed on the data, then the extracted components are used as independent variables in regression. According to the RMSEP and the R-squared, the first two components were used to build the model (Fig. 3). The R-squared value is 0.86. Training data is the sixty two modern endocasts from different region and testing the other thirty (Table 1).

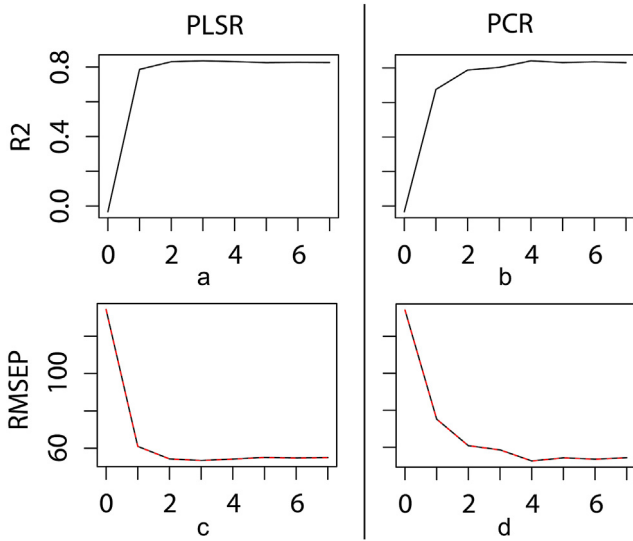


Fig. 3. Change in the R-squared values (a and b) and RMSEP (c and d) with the number of components (shown on the x-axis). The left side of the figure (a and c) shows the result of PLSR, and the right side (b and d) shows the result of PCR.

2.5. Blind tests

Blind tests were carried out on twenty Chinese and ten assorted modern human skulls and endocasts. The models were tested with data that were not used in building the models. First, the measurements on skulls and endocasts needed in the models were obtained. Then, the predictions of the cranial capacities were calculated using the models. Finally, the deviation was calculated by subtracting this estimate from the cranial capacity previously obtained using the virtual endocast. The same procedures were used on the fossil human specimens to obtain estimates and deviations, whereas the “real” cranial capacities were not obtained through the virtual endocasts but the water displacement method. Through blind test, we can predict the errors of the models when applied on unknown specimens. The results of blind test are reliable and replicable in future studies.

3. Results

3.1. Tests of the models

We use the mean ± standard deviation to evaluate the accuracy of each model with respect to modern human skulls or endocasts. The errors of the porion-vertex formula and the temporal lobe height formula are 5.49 ± 101.63 ml and 23.74 ± 83.8 ml, respectively. The errors of the multiple linear regression model for skulls and for endocasts are 2.8 ± 72.81 ml and 29.02 ± 58.96 ml, respectively (Fig. 4). The results show that endocast-based models are better than skull-based ones, especially for the multiple linear models. Additionally, we notice that the formulae obtained from skulls have less deviation from zero. This means that the models on skulls have a rather small systematic error, whereas the models based on endocasts are somewhat large. The reason might be that the vaguer landmarks of some endocasts make it more difficult to locate a standard position compared with skulls.

3.2. Comparison of SLR, MLR, PCR and PLSR

To compare the error of the different methods, the results of four endocast models are extracted. These four models are

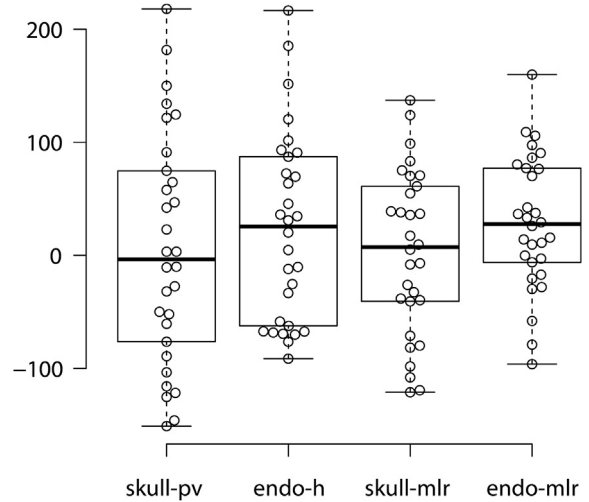


Fig. 4. Box-and-whisker plots of the errors of the formulae for skulls and endocasts.

Table 4
Predicted errors of the six models.

Model	Min	Max	Mean	SD
skull-pv	-151.05	217.81	5.49	101.63
skull-mlr	-121.09	137.17	2.80	72.81
endo-h	-91.32	216.39	23.74	83.80
endo-mlr	-96.16	159.84	29.02	58.96
endo-pcr	-90.57	119.32	17.44	53.81
endo-plsr	-70.30	118.76	20.44	48.27

representatives of four different statistical methods. Using the same data, we can directly analyze their advantages and disadvantages.

We use the mean ± standard deviation to evaluate their accuracies. Thus, the error values of the SLR, MLR, PCR and PLSR models are 23.74 ± 83.8 ml, 29.02 ± 58.96 ml, 17.44 ± 53.81 ml and 20.44 ± 48.27 ml (Table 4).

A small systematic error was observed because all four models generate a positive bias. The results show that SLR was the worst among them: the difference between the predicted cranial capacity and the actual capacity can reach up to 200 ml in the maximum

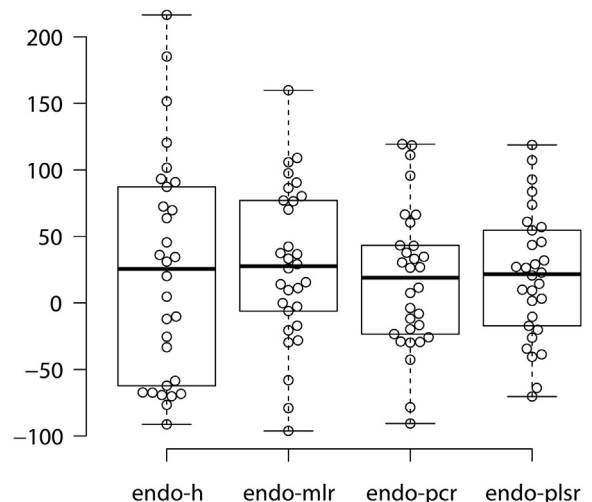


Fig. 5. Box-and-whisker plots of the errors of endocast models.

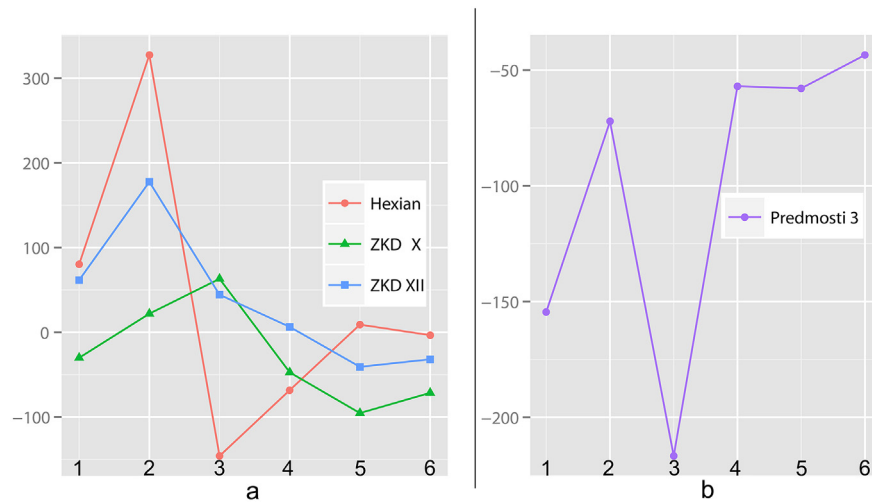


Fig. 6. Line chart of the prediction error for *Homo erectus* (left) and Late Pleistocene *Homo sapiens* (right). 1–6 are the six methods 1: skull-h, 2: skull-mlr, 3: endo-h, 4: endo-mlr, 5: endo-pcr, 6: endo-plsr.

case. In contrast, the other three models used more than one variable and performed better. Over 2/3 of the PLSR and PCR predictions deviate less than 50 ml. From this point of view, these two methods are much better than multiple linear regressions (Fig. 5).

3.3. Validation on fossil humans

To test the accuracy of these models in fossil humans, we chose several well-preserved fossil humans and measured both the skulls and the endocasts (Table 5). The predicted cranial capacity and the “real” cranial capacity based on manual reconstruction of the endocast are listed in Table 6. A line chart was made to clearly illustrate the results (Fig. 6).

Table 5
Measurements of the fossil humans.

Measurements		ZKD X	ZKD XII	Hexian	Predmosti 3
Skull	b-a	126.0	124.0	123.5	145.0
	ast-ast	111.0	115.0	141.8	106.0
	p-v	105.0	100.0	100.5	130.5
Endocast	arc b-l	93.5	103.6	118.0	136.0
	b-l	85.0	96.0	104.1	124.7
	b-a	108.8	105.6	124.6	137.8
	l-a	72.7	67.5	72.6	80.2
	l-o	29.9	37.4	32.2	31.1
	ast-ast	102.5	105.2	96.4	108.0
	h	96.2	87.3	111.8	117.8
	w-f	48.4	54.6	57.9	62.3
	w-endo	64.0	67.3	70.7	73.0

Table 6
Predictions for the fossil humans.

Specimen	re-endo	skull-pv	skull-mlr	endo-h	endo-mlr	endo-pcr	endo-plsr
ZKD X	1225	1195	1247	1288	1178	1130	1154
ZKD XII	1030	1092	1208	1074	1036	989	998
Hexian	1022	1102	1349	876	954	1031	1018
Predmosti 3	1670	1515	1597	1453	1613	1612	1626

Table 7
Cranial capacity of Jingchuan 1 using seven methods.

Specimen	re-endo	skull-pv	skull-mlr	endo-h	endo-mlr	endo-pca	endo-plsr
Jingchuan 1	1630	1505	1533	1468	1512	1470	1457

In the case of *H. erectus*, we can see that the estimates using endocasts are more reliable compared with those using skulls. Hexian is a special case because it has a rather wide biasterion width and a rather low temporal height. Thus, the skull-mlr and endo-h formulae that used these two features have rather large errors.

Predmosti 3 is a well-preserved Late *H. sapiens*. The estimate for Predmosti 3 using endocast-based formulae is more reliable (Table 6). Additionally, the 3rd method here, endo-h, used only the height of the temporal lobe and yielded a large error. Therefore, using only one variable may cause a fatal error in prediction.

3.4. Cranial capacity of Jingchuan 1

Using the skull-based models, the cranial capacity of Jingchuan 1 is 1505 ml and 1533 ml for the porion-vertex formula and the multivariate formula respectively. Using the endocast-based models, the cranial capacity of Jingchuan 1 is 1468 ml, 1512 ml, 1470 ml, and 1457 ml for the brain height formula, multiple linear model, PCR model and PLSR model, respectively. In addition to these six models, manual reconstruction is also used to estimate the cranial capacity of the Jingchuan 1 skull. However, the reconstruction is approximately 1600 ml, whereas other predictions are approximately 1500 ml. Thus, it differs from the other 6 methods by approximately 100 ml.

4. Discussion

4.1. Manual reconstruction of the endocast

Although manual reconstruction is the most common method used in paleoanthropology, there is no evidence that this type of method is highly accurate. When faced with poorly preserved skulls, the estimation becomes trickier, and the results will be unpredictable. For example, australopithecines Sts 71 and Stw 505 are partial crania and their cranial capacities have been estimated for many times. The cranial capacity of Sts 71 has changed from 428 ml to 370 ml, and then 414–430 ml by different correction for the deformation of the specimen (Holloway, 1970; Conroy et al., 2000, 1998). In this study, the reconstructed endocast of Jingchuan 1 does not appear to differ significantly from the original one visually, but the result differs greatly from the other models. One reason is that the frontal part is missing and reconstructed smoothly, which may

not correspond to the real shape of the original one. The other is that the basiocranial part of Jingchuan 1 is largely missing. Making plasticine endocasts without these details will inevitably affect the estimates on it. Thus, it is recommended here to use formulae-based methods rather than the manual reconstruction method to obtain the cranial capacity.

4.2. Comparison of the six models

The determination of cranial capacity is of great importance in the taxonomy of fossil men. Methods have been improving all the time in order to get a precise estimation on broken skulls (Tobias, 1964; Olivier and Tissier, 1975; Conroy et al., 2000). Two problems have always been essential in getting a more precise result: 1) the small sample size of fossils, 2) uncertainties of the required reconstruction (Neubauer et al., 2012).

Using modern humans as the training set and also for testing, we find that, overall, the accuracies of the estimates can reach a relatively high level. Models based on endocasts perform better than those based on skulls, and models using multiple variables have a higher accuracy than the univariate ones. Among the models that use more than one variable, PCR and PLSR are better than the traditional multiple linear regression models. Therefore, we recommend the multivariable models and endocast-based models for obtaining more precise estimates.

4.3. Cranial capacity estimated on fossil humans

The cranial capacities estimated for early fossil humans, such as Zhoukoudian and Hexian, are different from those of modern humans. Investigators have noticed long ago that formulae derived from modern external measurements are apt to overestimate the cranial capacity when used in fossils (Olivier and Tissier, 1975). Others have tried to subtract a constant number from the formulae in order to reduce the influence of the skull wall (Lee and Pearson, 1901; Dekaban, 1977). Compared with the external morphological features of early fossil humans, the endocranial morphology is less different from modern human. Thus, using models on endocasts are closer to the actual cranial capacity. Interestingly, when using 3 variables on the *H. erectus* skulls, the result is worse than the univariable porion-vertex formula, indicating that differences exist among most areas of the skull. Thus, more variables compounded the differences.

For the Late Pleistocene fossil skulls, the error of the cranial capacity of Predmosti 3 is small. The preservation of Predmosti 3, together with its endocast, is almost complete. Its skull and brain morphology are close to modern humans, thereby yielding a better prediction, especially with the endocranial models.

4.4. Interpretation of the errors

Although models can explain most of the variability in cranial capacity estimation, there are still many variables that cannot be included or factors relating to cranial capacity that are not fully explained. To obtain a better understanding of the error, we discuss the range of possible situations that can introduce error.

Although measurements on skulls or endocasts are related to cranial capacity, this correlation can never reach 100% because endocasts are not regular in geometry. Thus, error is unavoidable, and more variable endocasts are associated with greater inaccuracy in the predictions. Furthermore, modern humans vary significantly in terms of cranial shape and cranial capacity (Pearson, 1926; Tildesley, 1927; Acer et al., 2007; Nooranipour and Farahani, 2008). Thus, formulae cannot accurately predict them all.

The second consideration is preservation. Even with a complete skull, we can obtain different results using different methods. Some

skulls are complete outside but incomplete inside. Unfortunately, this type of incompleteness is less studied and always more neglected. In our study, the virtual endocasts were reconstructed from skulls in which only the intra-cranial wall were broken. However, using different types of parameters in the 3D reconstruction software, we can obtain a difference of up to 50 ml or more on one skull. Therefore, it is likely that greater uncertainties would be associated with situations in which the intra-structures are broken.

In addition, populations from different regions tend to have different cranial capacity distributions (Ricklan and Tobias, 1986; Hwang et al., 1995; Ilayperuma, 2011). Thus, using the 50 skulls and 62 endocasts as the modeling data still lacks reliability for application to all human populations.

5. Conclusions

Jingchuan 1 has a cranial capacity between 1457 ml and 1470 ml. The results are calculated through PLSR and PCR based on 62 modern endocasts. Blind tests on other modern skulls and fossil skulls have shown that the estimates of the PCR and PLSR models are quite reliable.

Comparisons between different methods have shown that a precise manual construction requires paleoanthropological knowledge and varies between reconstructions. Models using PCR and PLSR based on modern human endocasts can give a reliable result in predicting the cranial capacity of both modern and fossil humans and are much easier to accomplish. In the future, the cranial capacity of broken skulls can be calculated using these methods.

Acknowledgments

This work was supported by the Chinese Academy of Sciences (GJHZ201314, KZZD-EW-03, XDA05130102) and the National Natural Science Foundation of China (41272034 and 41302016). We thank Wu Liu and Emiliano Bruner for their helpful discussions and guiding.

References

- Acer, N., Usanmaz, M., Tugay, U., Erteki'n, T., 2007. Estimation of cranial capacity in 17–26 years old university students. *International Journal of Morphology* 25, 65–70.
- Bruner, E., Manzi, G., Arsuaga, J.L., 2003. Encephalization and allometric trajectories in the genus *Homo*: evidence from the Neandertal and modern lineages. *Proceedings of the National Academy of Sciences of the United States of America* 100, 15335–15340.
- Cameron, J., 1928. Correlations between cranial capacity and cranial length, breadth, and height, as studied in the Greenland Eskimo crania, United States National Museum. *Craniometric Studies*, No. 9. *American Journal of Physical Anthropology* 11, 259–268.
- Carrascal, L.M., Galván, I., Gordo, O., 2009. Partial least squares regression as an alternative to current regression methods used in ecology. *Oikos* 118, 681–690.
- Conroy, G.C., Weber, G.W., Seidler, H., Tobias, P.V., Kane, A., Brunson, B., 1998. Endocranial capacity in an early hominid cranium from Sterkfontein, South Africa. *Science* 280, 1730–1731.
- Conroy, G.C., Falk, D., Guyer, J., Weber, G.W., Seidler, H., Recheis, W., 2000. Endocranial capacity in *Sts 71 (Australopithecus africanus)* by three-dimensional computed tomography. *Anatomical Record* 258, 391–396.
- Dekaban, A.S., 1977. Tables of cranial and orbital measurements, cranial volume, and derived indexes in males and females from 7 days to 20 years of age. *Annals of Neurology* 2, 485–491.
- Ding, S., Yan, X., Fa, D., Ren, G., Xue, L., Lai, X., Wu, C., 1992. The improvement of the measurement and estimation of the cranial capacity. *Acta Anthropologica Sinica* 11, 241–249.
- Geladi, P., Kowalski, B.R., 1986. Partial least-squares regression: a tutorial. *Analytica Chimica Acta* 185, 1–17.
- Gil, J.A., Romera, R., 1998. On robust partial least squares (PLS) methods. *Journal of Chemometrics* 12, 365–378.
- Haack, D.C., Meihoff, E.C., 1971. A method for estimation of cranial capacity from cephalometric roentgenograms. *American Journal of Physical Anthropology* 34, 447–452.

- Hoadley, M.F., Pearson, K., 1929. On measurement of the internal diameters of the skull in relation: (I) to the prediction of its capacity, (II) to the "pre-eminence" of the left hemisphere. *Biometrika* 21, 85–123.
- Holloway, R.L., 1970. New endocranial values for the australopithecines. *Nature* 227, 199–200.
- Holloway, R.L., 2004. The Human Fossil Record, Brain Endocasts—the Paleoneurological Evidence, first ed. Wiley-Liss.
- Holloway, R.L., 1983. The O.H.7 (Olduvai Gorge, Tanzania) parietal fragments and their reconstruction: a reply to Wolpoff. *American Journal of Physical Anthropology* 60, 505–516.
- Holloway, R.L., 1973. New endocranial values for the East African early hominids. *Nature* 243, 97–99.
- Hwang, Y.I., Lee, K.H., Choi, B.Y., Lee, K.S., Lee, H.Y., Sir, W.S., Kim, H.J., Koh, K.S., Han, S.H., Chung, M.S., 1995. Study on the Korean adult cranial capacity. *Journal of Korean Medical Science* 10, 239–242.
- Ilayperuma, I., 2011. Cranial capacity in an adult Sri Lankan population: sexual dimorphism and ethnic diversity. *International Journal of Morphology* 29, 479–484.
- Isaza, J., Díaz, C.A., Bedoya, J.F., Monsalve, T., Botella, M.C., 2014. Assessment of sex from endocranial cavity using volume-rendered CT scans in a sample from Medellín, Colombia. *Forensic Science International* 234, 186.e1–186.e10. <http://dx.doi.org/10.1016/j.forsciint.2013.10.023>.
- Isserlis, L., 1914. Formulae for the determination of the capacity of the negro skull from external measurements. *Biometrika* 10, 188–193.
- Johnson, R.A., Wichern, D.W., 1992. *Applied Multivariate Statistical Analysis*. Prentice Hall Englewood Cliffs, NJ.
- Jolliffe, I.T., 1982. A note on the use of principal components in regression. *Journal of the Royal Statistical Society. Series C (Applied Statistics)* 31, 300–303.
- Jorgensen, J.B., Quaade, F., 1956. External cranial volume as an estimate of cranial capacity. *American Journal of Physical Anthropology* 14, 661–664.
- Kaufman, B., David, G.J., 1972. A method of intracranial volume calculation. *Investigative Radiology* 7, 533–538.
- Lee, A., Pearson, K., 1901. Data for the problem of evolution in man. VI. A first study of the correlation of the human skull. *Philosophical Transactions of the Royal Society A: Mathematical, Physical and Engineering Sciences* 196, 225–264.
- Li, H., Wu, X., Li, S., Huang, W., Liu, W., 2010. Late Pleistocene human skull from Jingchuan, Gansu Province. *Chinese Science Bulletin* 55, 1047–1052.
- Liu, Y., Chen, X., Ouyang, A., 2008. Non-destructive measurement of soluble solid content in Gannan navel oranges by visible/near-infrared spectroscopy. *Acta Optica Sinica* 28, 478–481.
- Liu, Y., Huang, W., Lin, Y., 1984. Human Fossil and Paleolithic Remains from Jingchuan, Gansu. *Anthropological Science*, pp. 11–90.
- Lockwood, C.A., 1999. Endocranial capacity of early hominids. *Science* 283, 9.
- Manjunath, K.Y., 2002. Estimation of cranial volume—an overview of methodologies. *Journal of the Anatomical Society of India* 51, 85–91.
- Márquez, S., Laitman, J.T., 2008. Climatic effects on the nasal complex: a CT imaging, comparative anatomical, and morphometric investigation of *Macaca mulatta* and *Macaca fascicularis*. *Anatomical Record* 291, 1420–1445.
- Mevik, B.H., Cedervik, H.R., 2004. Mean squared error of prediction (MSEP) estimates for principal component regression (PCR) and partial least squares regression (PLSR). *Journal of Chemometrics* 18, 422–429.
- Mevik, B.-H., Wehrens, R., 2007. The pls package: principle component and partial least squares regression in R. *Journal of Statistical Software* 18, 1–24.
- Mevik, B.-H., Wehrens, R., Liland, K.H., 2013. *Pls: partial Least Squares and Principal Component Regression*. R package version 2.
- Morton, S.G., 1849. Observations on the Size of the Brain in Various Races and Families of Man, Proceedings of the Academy of Natural Sciences of Philadelphia.
- Neubauer, S., Gunz, P., Weber, G.W., Hublin, J.J., 2012. Endocranial volume of *Australopithecus africanus*: new CT-based estimates and the effects of missing data and small sample size. *Journal of Human Evolution* 62, 498–510.
- Nguyen, D.V., Rocke, D.M., 2002. Tumor classification by partial least squares using microarray gene expression data. *Bioinformatics (Oxford, England)* 18, 39–50.
- Nooranipour, M., Farahani, R.M., 2008. Estimation of cranial capacity and brain weight in 18–22-year-old Iranian adults. *Clinical Neurology and Neurosurgery* 110, 997–1002.
- Olivier, G., Tissier, H., 1975. Determination of cranial capacity in fossil men. *American Journal of Physical Anthropology* 43, 353–362.
- Olivier, G., Aaron, C., Fully, G., Tissier, G., 1978. New estimations of stature and cranial capacity in modern man. *Journal of Human Evolution* 7, 513–518.
- Pearson, K., 1926. On the reconstruction of cranial capacity from external measurements. *Man* 26, 46–50.
- R Core Team, 2015. *R: a Language and Environment for Statistical Computing*.
- Ricklan, D.E., Tobias, P.V., 1986. Unusually low sexual dimorphism of endocranial capacity in a Zulu cranial series. *American Journal of Physical Anthropology* 71, 285–293.
- Stewart, T.D., 1934. Cranial capacity studies. *American Journal of Physical Anthropology* 18, 337–361.
- Tildesley, M.L., 1948. The waterproofing of a test skull and measurement of its water capacity. *Man* 48, 50–52.
- Tildesley, M.L., 1927. Determination of the cranial capacity of the negro from measurements of the skull of the living head. *Biometrika* 19, 200–206. <http://dx.doi.org/10.2307/2332183>.
- Tobias, P.V., 1964. The Olduvai Bed I Hominine with special reference to its cranial capacity. *Nature* 202, 3–4.
- Wang, H., 1999. *Partial Least Squares Regression: Method and Applications*. National Defence Industry Press, Beijing.
- Weber, G.W., Kim, J., Neumaier, A., Magori, C.C., Charles, B., Recheis, W., Seidler, H., 2000. Thickness mapping of the occipital bone on CT-data – a new approach applied on OH 9. *Acta Anthropologica Sinica* 19, 37–46.
- Weidenreich, F., 1937. Reconstruction of the entire skull of an adult female individual of *Sinanthropus pekinensis*. *Nature* 140, 1010–1011.
- Weidenreich, F., 1936. Observations on the form and the proportions of the endocranial casts of *Sinanthropus pekinensis*, other hominids and the great apes: a comparative study of brain size. *Palaeontologia Sinica, Series D* 7, 1–50.
- Wold, S., Ruhe, A., Wold, H., Dunn III, W.J., 1984. The collinearity problem in linear regression. The partial least squares (PLS) approach to generalized inverses. *SIAM Journal on Scientific and Statistical Computing* 5, 735–743.
- Wold, S., Sjöström, M., Eriksson, L., 2001. PLS-regression: a basic tool of chemometrics. *Chemometrics and Intelligent Laboratory Systems* 58, 109–130.
- Wolpoff, M.H., 1981. Cranial capacity estimates for Olduvai Hominid 7. *American Journal of Physical Anthropology* 56, 297–304.
- Wu, X., Liu, W., Dong, W., Que, J., Wang, Y., 2008. The brain morphology of Homo Liujiang cranium fossil by three-dimensional computed tomography. *Chinese Science Bulletin* 53, 2513–2519.